

# Nonlinear interaction of homogeneously oscillating domains in a planar gas discharge system

C. Strümpel, Yu. A. Astrov,\* and H.-G. Purwins

*Institute of Applied Physics, Münster University, Corrensstrasse 2/4, D-48149 Münster, Germany*

(Received 27 March 2000)

A planar dc gas discharge system with a high Ohmic semiconductor cathode is investigated with respect to temporal destabilization of the stationary homogeneous state. A subcritical Hopf bifurcation is observed, leading to a spatial homogeneous oscillation. The dependence of the oscillator's properties on control parameters is investigated. By applying spatial nonuniform optical control of the semiconductor cathode, several domains that may oscillate on different frequencies can be created. These spatially homogeneous domains can interact with each other through common boundaries. By adjusting the strength of coupling of the domains, their interaction can be controlled. In this interaction, regularities have been found that are, in some aspects, similar to those observed in externally driven nonlinear oscillators.

PACS number(s): 05.45.Xt, 52.80.-s

## I. INTRODUCTION

Systems that are capable of self-organized pattern formation are well known in different branches of science, among them biology, chemistry, and physics [1–4]. The evolving patterns can show a rather complicated spatiotemporal behavior. The first bifurcation from a stationary and spatial homogeneous state usually creates a relatively simple state. Frequently observed bifurcations are the Turing bifurcation leading to a spatial periodic pattern and the Hopf bifurcation. Undergoing a simple Hopf bifurcation, a system remains spatially homogeneous while it performs an oscillation in time.

Self-oscillating regimes of nonequilibrium spatially extended media are common in such diverse areas as the generation of pulses in the neuronal activity of the brain [5], the periodic variations of densities of biological species in ecosystems [6], oscillating modes of chemical reactions [7,8], and electrical networks [9]. To a large extent, the dynamics of these systems is determined by the cooperative movement of local oscillators in a spatially extended medium. One of the important phenomena that are observed in this context is the synchronization of local oscillators [10].

In the present work, we show that a dc-driven planar gas discharge device with a semiconductor gallium arsenide electrode operating at room temperature presents a flexible and experimentally convenient system to study the Hopf bifurcation in a spatially extended nonequilibrium media. At the studied set of experimental parameters, for the discharge in nitrogen a subcritical bifurcation to a homogeneously oscillating state has been revealed. The oscillation exists within a wide range of control parameters which determine its characteristic properties, such as frequency and amplitude. One of the control parameters is the conductivity of the semiconductor electrode. Due to the photosensitivity of the semiconductor, its conductivity can be controlled by irradiation with light. In contrast to other oscillating gas discharge devices (e.g., the one in Ref. [11]), several domains with oscillations

differing in amplitude and frequency can be established by applying a spatial nonuniform irradiation of the semiconductor. These domains can be separated from each other by nonoscillating regions and can act as independent oscillators. The strength of the interaction between these oscillators can be controlled by the width of the nonirradiated regions. When the separating regions are small or when they are not formed, a significant interaction between the oscillating domains can be observed, which results in a typical nonlinear behavior, such as periodic pulling and global synchronization.

It has been shown earlier that gas discharge systems similar to that studied in the present work at cryogenic temperatures ( $T \approx 90$  K) demonstrate the Turing instability as the first bifurcation from a homogeneous (reference) state [12–16]. We remark also that planar gas discharge systems with a semiconductor electrode can serve as fast converters of infrared images to the visible [17]. Therefore, studying the stability of their operation is important for these and other technical applications [18–20].

## II. EXPERIMENTAL SETUP

The experimental setup is sketched in Fig. 1. The studied system is essentially a sandwichlike structure composed of

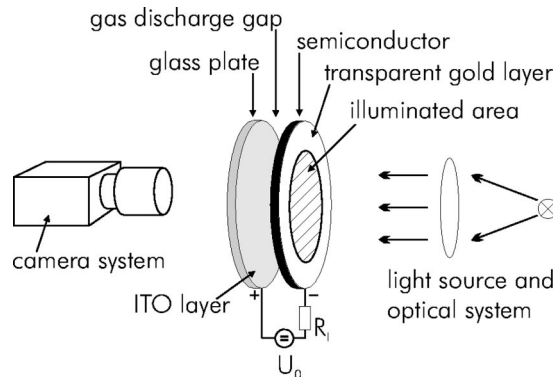


FIG. 1. Sketch of the experimental setup. The diameter of the discharge area is 30 mm, the width of the discharge gap is typically 0.5 mm. The device is filled with nitrogen at a typical pressure of 40 mbar.

\*Also at the A. F. Ioffe Physico-Technical Institute, Russian Academy of Sciences, St. Petersburg 194021, Russia.

parallel layers. The two parts mainly specifying the properties of the system are a semiconductor and a gas layer. In our case, the semiconductor material is semi-insulating gallium arsenide with a specific resistivity of  $2.6 \times 10^7 \Omega \text{ cm}$  [21]. The thickness of the semiconductor electrode is 1.5 mm.

Opposite to the semiconductor layer, there is a glass plate that is covered with a transparent and conductive indium tin oxide (ITO) layer. The space between the glass plate and the semiconductor is the gas layer. The discharge gap is filled with nitrogen; its width is typically changed in the range between 0.5 and 1.5 mm. In our case, the gas pressure is of the order of 40 mbar. The outer plane of the semiconductor wafer is covered with a gold film of a thickness of approximately 40 nm. Therefore, it is transparent to visible light with a transmission of about 10%. The sheet resistance of the ITO layer is in the range between  $15$  and  $20 \Omega/\square$  and that of the gold film is of the order of  $10 \Omega/\square$ . The resistances are negligible when compared with the sheet resistance of the gallium arsenide layer, which is  $1.7 \times 10^8 \Omega/\square$  in the non-irradiated case. The ITO and the gold electrode are connected to the external electric circuit, which consists of a dc high voltage supply  $U_0$  and a serial resistor  $R_I$  that is included to measure the current in the circuit.

Gallium arsenide is a direct semiconductor with a band gap of 1.42 eV at room temperature. When the radiation is absorbed, electrons are excited and perform transitions from the valence band to the conduction band. This internal photoeffect lowers the resistivity of the material. In our experiments, illumination from a halogen lamp was used. To ensure spatial homogeneous illumination, a homogeneous beam was prepared by a simple optical arrangement.

When the voltage supplied to the electrodes of the system is high enough, breakdown in the gas layer occurs. In the present experiments, the semiconductor layer acts as the cathode. The discharge can burn on a circular-shaped area with a diameter of 30 mm. In the following, this area is often referred to as the active area. The light that is emitted by the gas discharge can be observed through the ITO layer and the glass plate (cf. Fig. 1). The global light emission can be measured with a photomultiplier. The spatial distribution of the emitted light has been investigated by using an appropriate camera system. In the experiments, both a conventional CCD camera operating with videofrequency and a fast-gated intensified camera with a temporal resolution on the order of some 100 ns have been used.

The global discharge current is measured as the voltage drop at the serial resistor  $R_I = 100 \Omega$ . This voltage drop is negligible in comparison with the applied high voltage. Therefore, the voltage at the electrodes of the semiconductor gas discharge system is virtually equal to the applied voltage. The spatial distribution of the current density in the active area cannot be measured directly but it is proportional to the light density emitted by the discharge [15]. Therefore, measurements of the spatial distribution of discharge glow give also information about the corresponding behavior of the current.

### III. EXPERIMENTAL RESULTS

#### A. General features of the observed phenomena

Modern technology produces high-quality semiconductor materials, which provide high homogeneity of properties

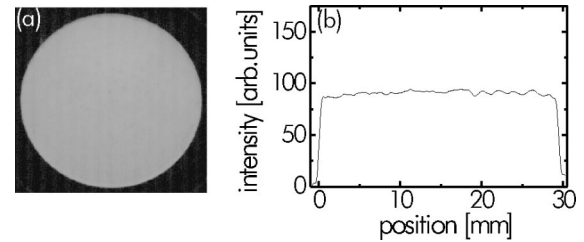


FIG. 2. Image (with 40 ms exposure time) of the stationary spatial homogeneous state of the gas discharge (a), which is used as a reference state, and a profile of the glow intensity along the horizontal diameter of the discharge channel (b). The experimental parameters are  $U_0 = 533 \text{ V}$ ,  $\phi_L = 0.94$ ,  $d = 0.5 \text{ mm}$ , and  $p = 47 \text{ mbar}$ . The active area has a diameter of 30 mm.

across wafers of a large diameter. The gallium arsenide wafers applied in the present research did not show any defects that would create essential inhomogeneities in the current density in the experimental system sketched in Fig. 1. Because of this, an electronic extended system with high homogeneity both of fixed and control parameters can be designed. At the appropriate set of experimental parameters, the stationary spatially homogeneous distribution of current is stable for low current density. At this state, the homogeneity of the initial (reference) state can be checked. The typical image of the discharge domain as well as the corresponding distribution of the glow intensity along the diameter of the discharge channel at these conditions are represented by Fig. 2.

Increasing the global current in the device either with the feeding voltage  $U_0$  or with the irradiating light flux  $\phi_L$  gives rise to the appearance of oscillations. They can be observed both in the discharge current and in the intensity of the discharge glow. The bifurcation to the oscillatory state creates a homogeneously oscillating state, which means that different parts of the extended system are phase-synchronized (cf. Sec. III B). The frequency depends on  $U_0$  and  $\phi_L$ . The photoelectrical control of the current density enables us to establish several domains in the extended system. Each of these domains is irradiated homogeneously but with an intensity that differs from that of other domains. Thus, different domains oscillate with different frequencies. The space between these domains can be kept at low current density, below the threshold for the bifurcation to oscillation. Such a geometry of the experiment leads to a study of the interaction of self-organized oscillating domains. Under these experimental conditions, it has been found that stronger oscillators (those with higher frequency and more dissipated electrical energy) pull weaker oscillators in a manner that is similar to that observed on externally driven oscillators (cf. Sec. III C).

As mentioned, the oscillation can be controlled by several parameters. One of the main control parameters is the discharge voltage  $U_0$ . The other one is the intensity  $\phi_L$  of the light, which is used to irradiate the semiconductor. In order to quantify this parameter, the influence of the incident light beam on the resistance of the semiconductor is measured. This has been done as follows. We assume that a homogeneous stationary Townsend discharge [22] is established in the gap at appropriate  $U_0$ . This mode of discharge is observed for low currents between the point of ignition and the

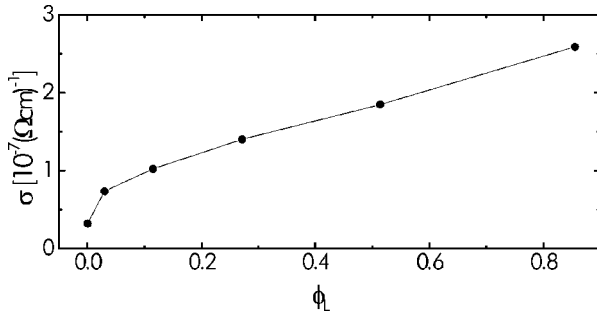


FIG. 3. Specific conductivity of the semiconductor layer as a function of the intensity of the irradiation.

point where negative differential conductivity is observed in the gas characteristic. An example is represented by the state shown in Fig. 2. The voltage-current characteristic  $U_0(I_D)$  of the device in this state yields a straight line, reflecting the Ohmic behavior of the semiconductor electrode (an example of such a characteristic in a similar system can be found in Ref. [23]). The voltage drop at the discharge gap for this discharge mode is independent of the current. Therefore, the slope of the  $U_0(I_D)$  characteristic provides the resistance of the gallium arsenide layer. Then, the specific conductivity can be computed from this resistance and the geometric dimensions. The conductivity as a function of the intensity of the irradiation is shown in Fig. 3, where  $\phi_L$  is normalized to the maximum output of the used light source. The conductivity of the semiconductor increases monotonically when the intensity of the irradiation is raised. In the considered experiments, the conductivity of the semiconductor electrode has been varied within approximately one order of magnitude. We remark that the dark conductivity (the case  $\phi_L = 0$ ) of  $3.85 \times 10^{-8} (\Omega \text{cm})^{-1}$  as it is given by the supplier [21] is near the measured value of  $3.2 \times 10^{-8} (\Omega \text{cm})^{-1}$ .

### B. Spatially synchronized oscillations

Spatial homogeneous oscillation occurs when the stationary homogeneous state is destabilized by increasing either the supply voltage  $U_0$  or the intensity of the irradiation  $\phi_L$ . The amplitude and frequency of the oscillation are independent of time when the control parameters remain fixed. This evidences the existence of an attractor of the system. The oscillation can be observed in the discharge current  $I_D$  as well as in the intensity of light  $\phi_G$  emitted by the gas discharge. This is demonstrated by typical time series of  $I_D$  and  $\phi_G$  that are shown in Figs. 4(a) and 4(b). The general shape of the signals is similar. However, they are not exactly in phase. The current reaches its maximum somewhat earlier than the discharge glow, whereas the falling edges of emitted light peaks are less steep when compared with the current peaks. This last phenomenon can be explained by the existence of the afterglow of the discharge. An example of the spectrum of the discharge current is shown in Fig. 4(c). The spectrum consists of a sequence of distinct peaks. In the case shown, the fundamental frequency is  $f_0 = 435$  kHz. The following peaks are higher harmonic components at integer multiples  $nf_0$  of the fundamental frequency. The spectrum of the emitted light (not shown here) is similar to that of the discharge current. The frequency of the oscillation depends on experimental control and fixed parameters. By altering

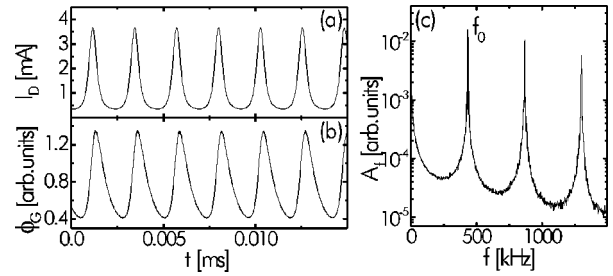


FIG. 4. Examples of a time series of the discharge current  $I_D$  (a) and of the intensity  $\phi_G$  of the light that is emitted by the gas discharge (b) in the oscillating state. The parameters are  $U_0 = 540$  V,  $\phi_L = 0.61$ ,  $d = 0.5$  mm, and  $p = 40$  mbar. Additionally, a spectrum of the discharge current is shown (c). The frequency is  $f_0 = 435$  kHz.

these parameters, the frequency can be typically changed in the range between 100 and 600 kHz, and the amplitude  $A(I_D)$  of the oscillation of the current (the difference between maximum and minimum values of the current) varies in the range between 0.5 and 4 mA. In this work, the properties of the oscillating system will be described by using the signal of the discharge current. Equivalently, the signal of the light intensity emitted by the discharge could be used, because the amplitude of its oscillation is proportional to that of the current when control parameters are varied.

When the active area of the device is halved, the oscillation persists with nearly unchanged frequency, while its amplitude decreases to approximately half of its initial value. This gives an indication that the oscillation is actually spatially homogeneous. The direct proof of the spatial homogeneity of the oscillating state is given by making snapshots of the discharge glow at different phases of an oscillation, see Fig. 5. The obtained images are rather noisy because of the necessity to keep short exposure times, whereas the intensity of the light emitted by the discharge is low. These data show that the discharge oscillates quite uniformly across the active area. The last picture shown in the sequence refers to a situ-

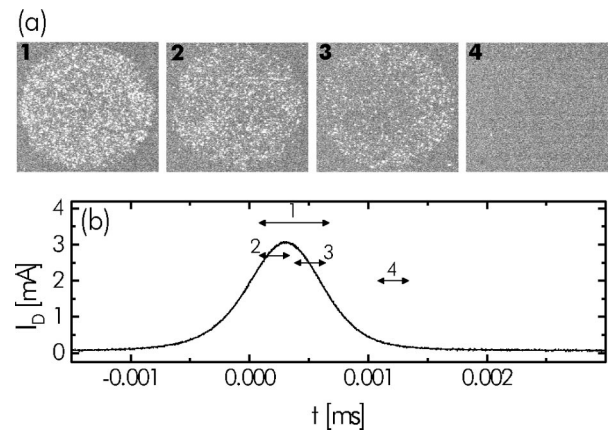


FIG. 5. Pictures taken with the intensifying camera during the rise and fall of one peak. The exposure times are 630 ns for picture (1) and 300 ns for pictures (2), (3), and (4). The position and length of the corresponding pulses, with which the camera is triggered, are marked in the oscilloscope trace for the current. The frequency of the oscillation is  $f_0 = 175$  kHz. The parameters are  $U_0 = 583$  V,  $\phi_L = 0.42$ ,  $d = 1$  mm, and  $p = 40$  mbar.

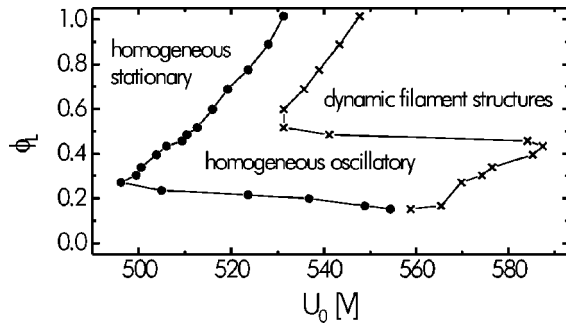


FIG. 6. Domain of existence of the homogeneous oscillation in the  $(U_0, \phi_L)$  parameter plane for  $p=40$  mbar and  $d=0.5$  mm. The circles denote the bifurcation from homogeneous stationary to homogeneous oscillatory states. The crosses indicate points of transition to spatial inhomogeneous structures.

ation where the current has nearly reached its minimum value. No significant emission of light could be recorded with the applied technique, while measurements with a photomultiplier tube give evidence of light emission on this stage [cf. Fig. 4(b)].

Homogeneous oscillations exist in a broad range of experimental parameters, see Fig. 6, where the domain of their existence in the control parameter plane  $(U_0, \phi_L)$  is shown. The full points indicate the subcritical bifurcation, which destabilizes the homogeneous stationary state in favor of the oscillatory state. A detailed description of the bifurcation is given in Fig. 7, where a typical example is presented. There, a hysteretic transition to the oscillatory state can clearly be noted when the irradiation of the semiconductor is used as a control parameter. A peculiarity of the system is that after the bifurcation to the oscillatory state, a further increase in the control parameter  $\phi_L$  leads to a transition back to the stationary state (cf. Fig. 6). This transition shows a hysteresis, too. The width of the hysteresis loops is approximately equal for both cases that are shown in Fig. 7. We note that the points in the map of Fig. 6 that mark the bifurcation to oscillation refer to an increase in the control parameters and that the bifurcation points are slightly shifted when compared with the corresponding ones in Fig. 7. This shift is probably due to aging processes of the semiconductor cathode because the two discussed measurements were done at different points in time.

In addition, data for bifurcations to more complicated structures are also shown in the map in Fig. 6. In most cases,

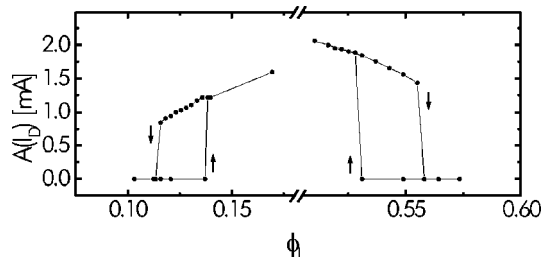


FIG. 7. An example of bifurcations from a stationary to an oscillatory state [with amplitude  $A(I_D)$ ] when  $\phi_L$  is varied while the supply voltage is fixed at  $U_0=510$  V. Two subcritical bifurcations are observed. The directions of change of the control parameter are indicated with arrows. The further parameters are  $d=0.5$  mm and  $p=40$  mbar.

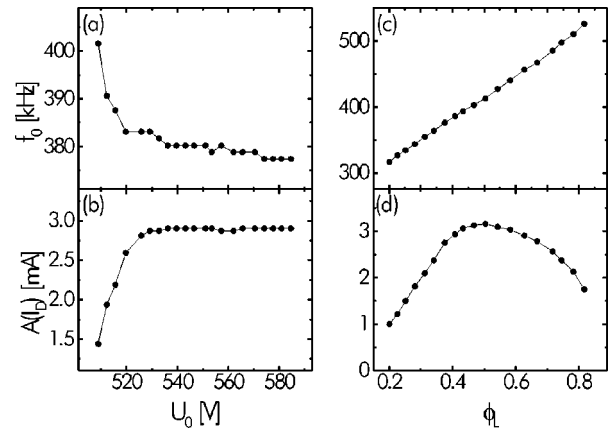


FIG. 8. Fundamental frequency  $f_0$  and amplitude  $A(I_D)$  of the oscillation along cross sections of the  $(U_0, \phi_L)$  parameter plane. For cases (a) and (b), the irradiation is kept constant at  $\phi_L=0.40$  and the voltage is increased. For cases (c) and (d), the voltage is kept constant at  $U_0=528$  V and the intensity of the irradiation is varied. In all cases the other parameters are  $p=45$  mbar and  $d=0.5$  mm.

these structures may be referred to as current filaments, which in our case are nonstationary, thus the state of spatially homogeneous oscillation is replaced by a complicated spatiotemporal pattern. The filamentary states usually appear when, starting from an oscillatory state, either the voltage or the irradiation of the semiconductor is increased. We remark that it is also possible to reach the spatially structured states without crossing the domain of the homogeneous oscillation. These direct transitions from the stationary homogeneous state require weak irradiations ( $\phi_L < 0.1$ ) of the semiconductor. Under these conditions, they take place at voltages between 550 and 600 V. The filamentary states themselves represent an interesting object to study, but a detailed discussion of these phenomena is beyond the scope of the present work.

In the parameter range of existence of the homogeneous oscillation, the dependence of the dynamical characteristics of the oscillating state on the experimental parameters can be investigated. While it is difficult to give a full description of the characteristics for the two-dimensional parameter space such as that depicted in Fig. 6, examples of data for two cross sections of this space are given in Fig. 8. Profiles along parallel cross sections are similar. Again, the hysteresis in the transitions is not shown; the data refer only to the increase in control parameters. Increasing the supply voltage  $U_0$  at constant irradiation of the semiconductor leads to a decrease in the frequency and an increase in the amplitude of the oscillation [Figs. 8(a) and 8(b)]. These regularities are expressed near the bifurcation point. At a further increase of the voltage, a tendency for saturation of both the frequency and the amplitude is observed. The variation of the irradiation of the semiconductor at a constant value of the supply voltage gives rise to an increase in the frequency of the oscillation, while the amplitude changes nonmonotonously. Just after the bifurcation to the oscillatory state, the amplitude grows, and after passing a maximum, it decreases until the transition back to the stationary state takes place [Figs. 8(c) and 8(d)].

The characteristics of the oscillating system also depend on other parameters of the device such as the discharge gap

width  $d$  and the gas pressure  $p$ . However, there exists a rather broad range of these parameters where the characteristics of the oscillation vary only slightly. For example, for  $d=0.5$  mm, variations in  $p$  between 25 and 55 mbar give only slight changes in the frequency and the amplitude of the oscillation. When  $p$  becomes smaller than 20 mbar, a significant decrease of the amplitude can be noted (of about 50%), while the frequency is only marginally affected (it varies by less than 5%).

The thickness of the discharge gap has an influence on the properties of the oscillation, too. For larger gaps, while other conditions remain unchanged, the frequency diminishes. For example, at  $d=0.5$  mm the typical range of frequency is from 250 to 600 kHz. When the gap is increased to  $d=1$  mm, the frequency range drops to values between 100 and 250 kHz. If the gap is made very large (e.g.,  $d>2$  mm), the oscillation ceases to exist. The amplitude of the oscillation decreases when increasing  $d$ . For example, the largest amplitude, which has been observed at  $\phi_L=1$  for  $d=1$  mm, is 2.5 mA, whereas under the same conditions the maximum amplitude for  $d=0.5$  mm is 4 mA.

### C. Interaction of domains oscillating on different frequencies

Due to the application of photoelectrical control of the semiconductor's conductivity, it is possible to create several spatially extended homogeneous domains with different local conductivity in the gas discharge device. In the preceding section, it has been shown that the conductivity influences the frequency of the oscillation. Therefore, each domain will oscillate on its own frequency. In order to suppress the interaction of neighboring oscillating domains, they can be separated by nonirradiated parts of the semiconductor electrode, which have to be broad enough. In this way, an ensemble of noninteracting oscillators can be created. Then, the width of the interfacial domains may be decreased to the extent needed to activate the coupling of oscillators. In the experiments described in this section, systems containing two and three oscillating domains have been studied. To reach an appropriate configuration, the formerly homogeneously irradiated semiconductor is now irradiated with a light beam that has a nonuniform cross section. This is reached by introducing an array of optical neutral filters into the homogeneous light beam. In this way, the semiconductor electrode is excited by a nonhomogeneous optical pattern that is projected onto it. The filters have transparencies in the range 50–90%. To create the nonactivated (separating) domains, the light beam is covered at appropriate areas. As a result of the variation of the coupling strength of neighboring oscillating domains, the frequency characteristic of the whole system is changing. The measurements presented here have been carried out at constant values of supply voltage  $U_0=540$  V and irradiation intensity  $\phi_L=0.61$ .

Figure 9(a) illustrates the situation where two different oscillating domains are established in the device. There, a picture of the gas discharge area made with a CCD camera is shown. The dark stripe on the image shows the position and the width of the nonirradiated stripe-shaped domain. In the case shown, the irradiation of the left side is 64% of that of the right side (which is  $\phi_L=0.61$ ). This leads to a significantly lower fundamental frequency for the left side, while

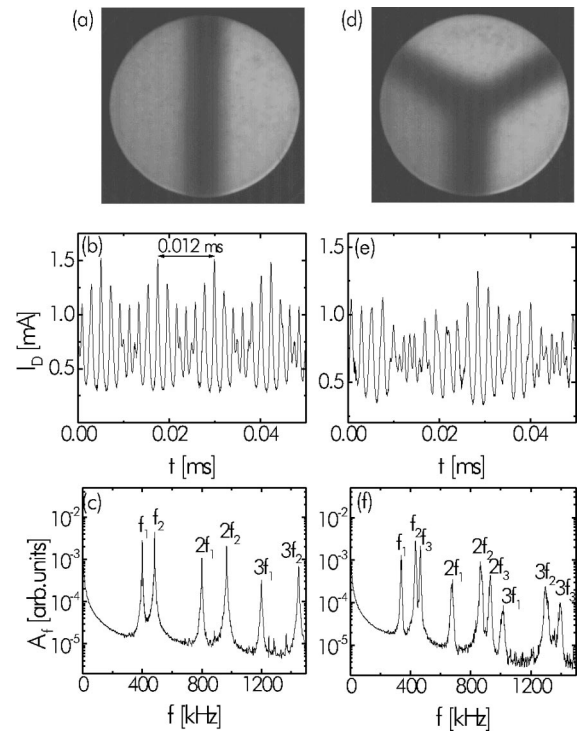


FIG. 9. Examples for the situation in which the system contains two or three different oscillating domains. The domains are separated by nonirradiated areas. The presence of two oscillators is illustrated by the picture of the gas discharge glow (a), the corresponding time series of the global discharge current (b), and the spectrum (c). The values for the irradiation are 0.39 and 0.61 for the left- and for the right-hand side, respectively. The situation of three different oscillating domains is illustrated by the picture of the discharge glow (d) and the corresponding time series (e) and spectrum (f). Here the values for the irradiation are 0.32 for the lower left, 0.55 for the upper, and 0.61 for the lower right part, respectively. For both cases, the further parameters are  $U_0=540$  V,  $d=0.5$  mm, and  $p=45$  mbar.

the amplitude is only slightly lower than that of the right side [cf. the profile in Fig. 8(d)]. An example of the time series of the global current is shown in Fig. 9(b) and the corresponding spectrum in Fig. 9(c). In the global spectrum, two fundamental frequencies can be recognized in the present case at  $f_1=399$  kHz and  $f_2=483$  kHz. The lower frequency  $f_1$  can be assigned to the domain with weaker irradiation, while the higher frequency  $f_2$  belongs to the stronger irradiated domain. There are also distinguished peaks at integer multiples of these fundamental frequencies. This spectral characteristic indicates a linear superposition of two oscillators that are formed by the two different domains in the system. This is confirmed by the time series of Fig. 9(b), which clearly shows beating of the two oscillators (the beat frequency is the reciprocal of the distance between two successive peaks with maximum amplitude). As follows from these data, the beat period is approximately 0.012 ms; this corresponds to a beat frequency of 82.4 kHz. This value is in good agreement with the difference between the two fundamental frequencies in the spectrum of Fig. 9(c),  $\Delta f=f_2-f_1=84$  kHz.

The case of three separated oscillating areas is demonstrated by the image of the discharge in Fig. 9(d). For the situation shown, the lower right part is irradiated with a

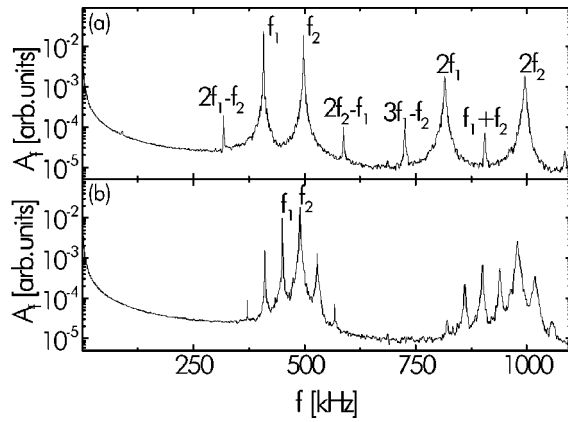


FIG. 10. Dependence of the spectrum of the total discharge current on the coupling between two oscillating domains. The width of the separating (dark) stripe is  $b=3$  mm (a) and  $b=0$  mm (b). The values for the irradiation are 0.39 and 0.61 for the left- and for the right-hand side, respectively. The fundamental frequencies are  $f_1=408$  kHz,  $f_2=498$  kHz in the first case (a) and  $f_1=450$  kHz,  $f_2=489$  kHz in the second case (b). The further parameters are the same as in Fig. 9.

filter, the irradiation of the lower left part is 52% and that of the upper part is 90% of the illumination of the lower right part (which is again  $\phi_L=0.61$ ). While the time series of the discharge current recorded for these conditions [Fig. 9(e)] demonstrates no clear regularities, the spectrum of the signal [Fig. 9(f)] indicates the linear superposition of three oscillators with different frequencies. Three fundamental frequencies  $f_1=339$  kHz,  $f_2=433$  kHz, and  $f_3=466$  kHz can be noted in the spectrum, together with the higher harmonic components at multiple integers of the fundamental frequencies. The upper part of the structure [Fig. 9(d)] oscillates on the frequency  $f_2$ . For the demonstrated case, it is close to the frequency  $f_3$ , which belongs to the lower right part, because the irradiations of both parts differ only slightly. The irradiation of the lower left part is much weaker. Therefore, its fundamental frequency  $f_1$  is clearly separated from the two other fundamental frequencies.

In both cases of two and three different oscillating domains, an interaction of the oscillations was suppressed by separating the neighboring homogeneous areas by nonirradiated stripe-shaped domains. By making the separating areas narrower, it is possible to gradually introduce an interaction between the neighboring oscillators. In the cases illustrated in Figs. 9(a) and 9(d), the width  $b$  of the separating stripe is 6 mm. In Fig. 10, the spectra of the discharge current for the cases  $b=3$  mm and  $b=0$  mm for the system with two oscillators are presented. These studies show that, when the separation of oscillating domains decreases, the oscillators begin to interact with each other. This can be detected via the occurrence of additional components in the spectra at frequencies  $nf_1 \pm mf_2$  (where  $n, m$  are small integer numbers). Some of these components are marked in Fig. 10(a). They appear due to the nonlinear interaction between the two oscillators. When the interaction becomes very strong (the case of no separation between the two oscillating domains), the spectrum has the shape shown in Fig. 10(b). As compared to the case of small interaction, the frequency  $f_1$  now has been pulled towards  $f_2$ . At the same time, the spectrum shows an

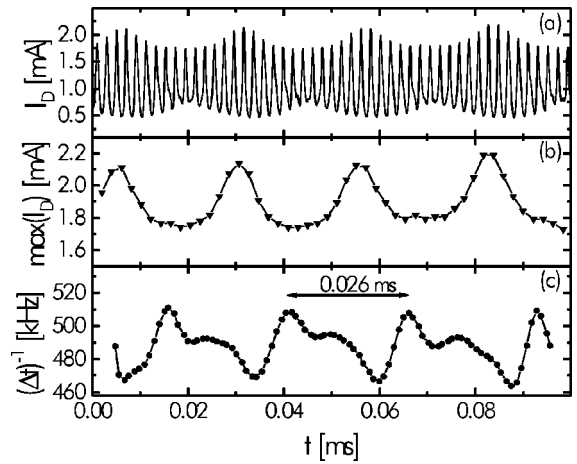


FIG. 11. An example of time series of the total discharge current in the absence of a separating stripe ( $b=0$  mm) (a), from which the spectrum in Fig. 10(b) is derived. To demonstrate the simultaneous amplitude and frequency modulation due to the interaction of the two domains, the maximum of each peak  $\max(I_D)$  (b) and the instantaneous frequency  $(\Delta t)^{-1}$  (c) as functions of time are shown.

asymmetry with respect to  $f_2$ , namely, the components at lower frequencies  $f < f_2$  are stronger than those at higher frequencies  $f > f_2$ . This behavior is characteristic for periodic pulling [24], which can occur at an incomplete entrainment of a nonlinear oscillator by an external harmonic driving force near an area of total frequency synchronization (also called Arnol'd tongue). The time series, from which the spectrum has been calculated [see Fig. 11(a)], shows nonlinear beating with a period that is again determined by the difference between the fundamental frequencies in the spectrum, which is  $f_2 - f_1 = 39$  kHz. To demonstrate the simultaneous anharmonic modulation of amplitude and frequency of  $I_D(t)$ , the envelope of the time series is plotted in Fig. 11(b) as a function of time. The modulation of the frequency can be seen when the instantaneous frequency is plotted as a function of time. Information about this frequency can be obtained from the distances  $\Delta t$  between successive zero points of a time series, which have the same sign of the first derivative [25]. In our case, the time series  $I_D(t) - \langle I_D(t) \rangle$  has been used to calculate the instantaneous frequency  $(\Delta t)^{-1}$ , which is plotted as a function of time in Fig. 11(c). In the example considered, both the amplitude and the frequency are modulated with a period of 0.026 ms; the frequency is 38.5 kHz.

The spectra shown in Figs. 9(c) and 9(f) reveal that, as the width of the separating stripe decreases, the frequency  $f_1$  shifts towards  $f_2$ , while  $f_2$  remains nearly unchanged. A quantitative measurement of this effect is given in Fig. 12. It is interesting to note that the shift of  $f_1$  can be detected even when the spectrum of the current does not show a clear sign of the nonlinear interaction. At the same time, it becomes more pronounced when the additional components due to the nonlinear interaction begin to emerge in the spectrum. For the conditions of getting the data in Fig. 12, it occurs at  $b \approx 4$  mm. Interpreting these results, the oscillator operating on the frequency  $f_2$  can be considered as a driving oscillator, which tries to entrain the neighboring oscillator having the lower fundamental frequency  $f_1$ . In the course of this synchronization process, the frequency of the driven oscillator is

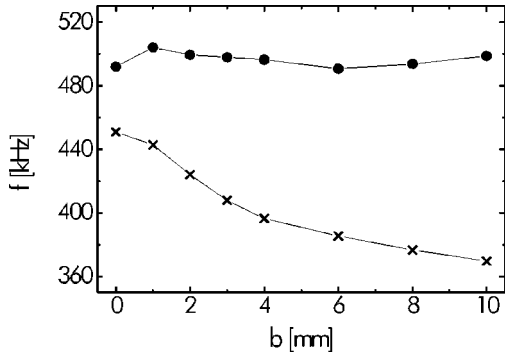


FIG. 12. The two fundamental frequencies  $f_1$  ( $- \times -$ ) and  $f_2$  ( $- \bullet -$ ) in the spectrum of the total discharge current of two oscillating areas as a function of the width  $b$  of the separating nonirradiated domain. The parameters are the same as for Fig. 9.

shifted towards the driving frequency.

While in the experiments described above the effect of a nonlinear influence of a stronger oscillator on a weaker one is observed, the complete synchronization of the two oscillating domains has not been registered. This may be related to the large difference  $\Delta f$  of their fundamental frequencies. In other experiments, when the value of  $\Delta f$  is decreased, the effect of global synchronization of the interacting oscillators can be observed. This is demonstrated on the system containing two domains of equal size (domains 1 and 2). The irradiation  $\phi_{L,1}$  of the first domain is varied while the excitation  $\phi_{L,2}$  of the second domain is kept at a constant level, which is always larger than that of the first domain ( $\phi_{L,1}/\phi_{L,2} \leq 1$ ). In the absence of interaction, the states of the two subsystems vary in a simple way, as the ratio  $r_\phi = \phi_{L,1}/\phi_{L,2}$  is changed—see curves  $f_1^0(r_\phi)$  and  $f_2^0(r_\phi)$  in Fig. 13. The frequencies  $f_1^0$  and  $f_2^0$  are measured for the case where only domain 1 or domain 2, respectively, is irradiated with the according intensity, while the other domain is in the stationary homogeneous state (without irradiation). For maximum interaction ( $b=0$ ) of the oscillators, a complicated dependence of the global dynamical properties of the

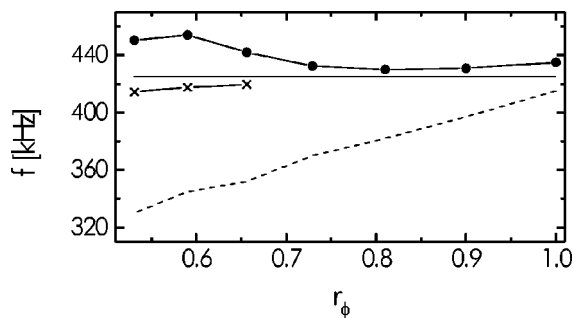


FIG. 13. Internal synchronization of two oscillating domains.  $f_1^0$  (dashed line) and  $f_2^0$  (straight line) are the fundamental frequencies of the unperturbed oscillation of the domains, which are irradiated with intensities  $\phi_{L,1}$  and  $\phi_{L,2}$ , respectively.  $f_1'$  (denoted by  $- \times -$ ) and  $f_2'$  (denoted by  $- \bullet -$ ) are the main frequencies from the spectra that result from the nonlinear interaction of the oscillating domains.  $r_\phi$  denotes the ratio  $\phi_{L,1}/\phi_{L,2}$ . The two domains are in direct contact with each other (the width of the nonirradiated area is  $b=0$  mm). The further parameters are  $U_0=540$  V,  $d=0.5$  mm, and  $p=45$  mbar.

system on the ratio  $r_\phi$  is observed—see the curves  $f_1'(r_\phi)$  and  $f_2'(r_\phi)$  in Fig. 13. There,  $f_1'$  and  $f_2'$  are the fundamental frequencies in the spectra of the global current. At a large value of  $\Delta f = f_2^0 - f_1^0$  (caused by a small ratio  $r_\phi$ ), the system's spectra resemble the one shown in Fig. 9(c); their asymmetry evidences the periodic pulling regime. There, the lower frequency  $f_1'$  is pulled towards  $f_2'$ . The interaction of the oscillators influences also the frequency of the “stronger” oscillator, which is shifted to higher values. In the course of increasing  $r_\phi$  and decreasing  $\Delta f$ , the frequency component of the pulled oscillator disappears. For the considered case, this occurs at  $r_\phi \approx 0.65$ . The spectra now contain only the fundamental frequency  $f_2'$  and its higher harmonics. This indicates the establishing of the global synchronization in the system, a state where it oscillates on the frequency of the stronger oscillator, although the external photoelectrical control is applied in a spatially nonhomogeneous way.

#### IV. DISCUSSION AND CONCLUSION

The discharge current in the dc-driven planar semiconductor gas discharge system under consideration is able to perform self-organized nonlinear oscillations. The fundamental frequency and the amplitude of the oscillation can be controlled by the supply voltage and by the irradiation of the semiconductor.

To understand the basic mechanism of the homogeneous oscillation, one should consider the different current-voltage characteristics of the two essential layers of the system. The semiconductor has a linear characteristic when the electric field is weak enough. For the gas discharge we operate the device up to the current range where the nonlinear characteristic has a negative slope due to the transition from low current Townsend discharge (at the voltage  $U_T$  across the gap) to high current glow discharge (at the voltage  $U_{\text{glow}}$  across the gap). In the present experiment, an important requirement for the occurrence of instability is that the operating point of the gas discharge is shifted towards the region where the slope of the characteristic becomes negative. The operating point is defined by the intersection of the load line  $U = U_0 - R_{\text{SC}} I_D$  with the discharge characteristic, where  $R_{\text{SC}}$  is the resistance of the active area of the semiconductor electrode (cf. Fig. 14). Thus, the destabilization can be achieved by increasing the supply voltage  $U_0$  or by decreasing the resistance  $R_{\text{SC}}$  by intensifying its irradiation. For example, in Fig. 14 the operating point  $O1$  is shifted to the point  $O2$  by increasing the voltage. Due to the negative differential resistance of the discharge characteristic, in the present experiment the current can increase while the voltage across the gap decreases. Because the voltage  $U_0$  at the outer metallic electrodes of the system is fixed, this leads to a rise of the voltage  $U_{\text{SC}}$  across the semiconductor which leads to a higher current. The increase of the current due to this positive feedback mechanism is restricted. When the voltage at the gap falls below  $U_{\text{glow}}$ , the discharge cannot be sustained any more. Therefore,  $U_{\text{SC}}$  cannot exceed  $U_0 - U_{\text{glow}}$  and, consequently, the current is limited. If the requirements for a stable glow discharge are fulfilled, it has to carry the current defined by  $U_{\text{SC}}$  (e.g., at the operating point  $O2$  in Fig. 14). Usually, a glow discharge adapts its lateral extension to meet

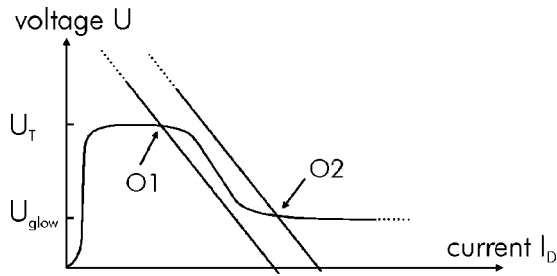


FIG. 14. Sketch of the static current-voltage characteristic of a gas discharge containing the Townsend and the glow discharge regime. The operating points are defined by the intersection with the load line, which is determined by the resistance of the semiconductor electrode and the feeding voltage. Two different load lines at two different voltages are included here with operating points in the Townsend regime ( $O1$ ) and the glow discharge regime ( $O2$ ), respectively. The stability of the operating points is discussed in the text.

the conditions, because the current density at the cathode is constant [22]. The experimental results show that this does not happen in our case. Instead, the transition to the high current state does not result in a stable state and the discharge is extinguished and  $I_D$  as well as  $U_{SC}$  are decreasing. A new Townsend discharge is ignited when the voltage at the gap reaches  $U_T$ , and the process can be repeated.

By taking the above mechanism into account, some of the features of the oscillation can be explained. Intensifying the irradiation in an oscillatory state should increase the amplitude of the oscillation. In our case, a monotonic rise can be found at rather weak irradiations. Increasing the voltage at a constant irradiation should also result in a larger amplitude. Indeed, in our case, the amplitude initially increases with the voltage. The constant level that it finally reaches indicates that the current is limited by another mechanism, which may be related to the metal semiconductor junction that is formed by the gold film on the gallium arsenide electrode.

The possibility of controlling the fundamental frequency of the oscillation with the irradiation of the semiconductor allows us to establish a number of domains with different frequencies by applying spatial nonhomogeneous irradiation. If they are spatially separated by domains that are nonactivated with light and are broad enough, the oscillating domains become independent of each other. On the other hand, when they are able to interact, scenarios which are known from driven nonlinear oscillators can be observed. Therefore, the interaction of two oscillators in the system can be described in general terms of nonlinear dynamics without considering the specific origin of the oscillators. A weak interaction leads to a quasiperiodic state, which is indicated by additional components in the spectrum. When the interaction becomes more intense, the stronger oscillator shifts the frequency of the weaker oscillator towards that of the strong one. Depending on the difference  $\Delta f$  between the two noninteracting domains, there are different final states when the interaction becomes strongest. In the case of a large initial  $\Delta f$ , the final state is characterized by periodic pulling [24], a state that can also be observed, e.g., at driven van der Pol-like oscillators near their point of synchronization [26]. In general, the driver is an external oscillation, while in some cases, the interaction of two internal oscillators has been ob-

served [25,27]. In the case of small initial  $\Delta f$ , we observe entrainment, where both domains oscillate with the same frequency. This effect offers an explanation for the homogeneity of the oscillation described in Sec. III B. Although in this case the system is excited homogeneously, there are always small unavoidable inhomogeneities. When the active area is divided into a large number of small domains, each of them would oscillate on a slightly different frequency than its neighbors. But the experiments show that these “local” oscillators are able to synchronize, thus performing a common oscillation that is, despite small inhomogeneities, homogeneous across the complete area. In spite of the large interest in studying the collective behavior of ensembles of oscillating systems in a homogeneous medium, which is mainly reflected in theoretical research (see, e.g., [28]), experimental data on the subject have been rather scarce up to now. Partly, this may be related to the lack of proper physical objects which could provide the needed experimental flexibility. We believe that the experimental system applied in this work enables us to carry out an extensive study of the problem.

The synchronous oscillation in different points of the spatially extended system suggests the existence of a mechanism of efficient phase synchronization. The simple semi-phenomenological reaction-diffusion model for the processes in a semiconductor gas discharge system that has been proposed in [14] suggests that two variables are included: the concentration of charge carriers in the discharge gap and the voltage drop on the semiconductor electrode. The lateral coupling is provided by diffusional spreading of both of these variables. It follows from the geometry of the studied layer system that the characteristic length of the lateral propagation of the potential should be of the order of the thickness of the system, which in our case is 2 mm. This value of the characteristic length is in correspondence with the observed distance between separately oscillating domains, when their interaction becomes essential (cf. Sec. III C). Such a mechanism of diffusional coupling turns out to be quite efficient, providing a complete spatial phase synchronization of oscillations in the homogeneously excited system.

In relation to the results in the present work, we notice that the very similar cryogenic semiconductor gas discharge device [13] demonstrates a Turing bifurcation as the first mechanism of destabilization of the spatially homogeneous stationary state of the discharge. The semiconductor material for the electrode in this case has been silicon doped with zinc. The observed behavior has been in correspondence with the reaction-diffusion model of [14] at some set of theoretical parameters. On the other hand, it has been theoretically established that, depending on the parameters of the problem, the first bifurcation can be either Hopf or Turing [29]. We believe that it is the dynamical properties of the discharge that are dependent on the gas temperature, and that are responsible for the qualitative difference in pattern formation phenomena as it is observed at cryogenic and room temperatures. In the course of taking preliminary measurements in a cryogenic device with a gallium arsenide electrode, a bifurcation to an oscillation has not been found. Instead, the reference state is spatially destabilized. To gain more detailed information on the role of temperature, further experimental investigations are needed.

To gain further insight into the theoretical description of semiconductor gas discharge systems, the reaction-diffusion equation used in [29] shall be discussed. It is a two-component equation for the current density and the voltage at the gas gap. This equation can be derived by modeling the experimental system with the help of discrete components such as Ohmic and nonlinear resistors, capacities, and inductivities [30]. The equation enables us to describe many features of gas discharge systems in a qualitative way. If we believe that this equation also describes the present experiment qualitatively, some conclusions with respect to the kind of bifurcations that occur can be drawn. The analysis of the stability of the homogeneous stationary state gives the following results [31]. In general, the state can be destabilized via the homogeneous or, alternatively, via a spatial periodic mode. In the first case, we deal with a Hopf bifurcation, in the second with a kind of Turing bifurcation. Both bifurca-

tions can be of supercritical or subcritical nature, depending on the system parameters. A decision as to which kind of bifurcation takes place is not possible for the present situation because this will be dependent on details of the parameters entering the model. The determination of the parameters of the equation from the experimental parameters cannot be made with sufficient precision because too many approximations have been made in the model. We believe that for a quantitative description of the gas discharge system considered, a model similar to that used to explain pattern formation in ac gas discharge systems [32,33] is appropriate.

#### ACKNOWLEDGMENTS

The support of the present work by the Deutsche Forschungsgemeinschaft (DFG) is gratefully acknowledged.

- 
- [1] H. Meinhardt, *Models of Biological Pattern Formation* (Academic Press, London, 1982).
- [2] *Chemical Waves and Patterns*, edited by R. Kapral and K. Showalter (Kluwer, Dordrecht, 1995).
- [3] F. H. Busse and S. C. Müller, *Evolution of Spontaneous Structures in Dissipative Continuous Systems* (Springer, New York, 1998).
- [4] H.-G. Purwins, Yu. A. Astrov, and I. Brauer, Proceedings of the 5th ECC, Orlando, 1999 (World Scientific, Singapore, in press).
- [5] H. Haken, *Principles of Brain Functioning: A Synergetic Approach to Brain Activity, Behavior and Cognition* (Springer, Berlin, 1996).
- [6] J. D. Murray, *Mathematical Biology* (Springer, Berlin, 1989).
- [7] *Chemical Oscillations, Waves, and Turbulence*, edited by Y. Kuramoto (Springer, Berlin, 1984).
- [8] *Oscillations and traveling waves in chemical systems*, edited by R. J. Field and M. Burger (Wiley, New York, 1985).
- [9] H.-G. Purwins and C. Radehaus, in *Pattern Formation on Analogous Parallel Networks*, edited by H. Haken, Springer Series on Synergetics Vol. 42 (Springer, New York, 1988).
- [10] S. H. Strogatz and R. E. Mirollo, *Physica D* **31**, 143 (1988).
- [11] P. R. Sasi Kumar, V. P. N. Nampoore, and C. P. G. Vallabhan, *Phys. Lett. A* **196**, 191 (1994).
- [12] Yu. A. Astrov, E. Ammelt, S. Teperick, and H.-G. Purwins, *Phys. Lett. A* **211**, 184 (1996).
- [13] E. Ammelt, Yu. A. Astrov, and H.-G. Purwins, *Phys. Rev. E* **55**, 6731 (1997).
- [14] Yu. A. Astrov and Yu. A. Logvin, *Phys. Rev. Lett.* **79**, 2983 (1997).
- [15] E. Ammelt, Yu. A. Astrov, and H.-G. Purwins, *Phys. Rev. E* **58**, 7109 (1998).
- [16] Yu. A. Astrov, I. Müller, E. Ammelt, and H.-G. Purwins, *Phys. Rev. Lett.* **80**, 5341 (1998).
- [17] L. M. Portsel, Yu. A. Astrov, I. Reimann, E. Ammelt, and H.-G. Purwins, *J. Appl. Phys.* **85**, 3960 (1999).
- [18] B. G. Salamov, S. Ellialtioglu, B. G. Akinoglu, N. N. Lebedeva, and L. G. Patriskii, *J. Phys. D* **29**, 628 (1996).
- [19] B. G. Salamov, S. Büyükkakç, M. Özer, and K. Çolakoğlu, *Eur. Phys. J.: Appl. Phys.* **2**, 275 (1998).
- [20] M.-G. Meisel and H. Langhoff, *Appl. Phys. B: Lasers Opt.* **64**, 41 (1997).
- [21] Material supplied by Freiburger Compound Materials GmbH (Germany) has been used.
- [22] Yu. P. Raizer, *Gas Discharge Physics* (Springer, Berlin, 1991).
- [23] L. M. Portsel, Yu. A. Astrov, I. Reimann, and H.-G. Purwins, *J. Appl. Phys.* **81**, 1077 (1997).
- [24] H. Lashinsky, in *Symposium on Turbulence of Fluids and Plasmas*, edited by J. Fox (Polytechnic, Brooklyn, NY, 1968), p. 29.
- [25] H. Klostermann, A. Rohde, and A. Piel, *Phys. Plasmas* **4**, 2406 (1997).
- [26] T. Klinger, A. Piel, F. Seddighi, and C. Wilke, *Phys. Lett. A* **182**, 312 (1993).
- [27] M. E. Koepke, T. Klinger, F. Seddighi, and A. Piel, *Phys. Plasmas* **3**, 4421 (1996).
- [28] S. H. Strogatz, *Nonlinear Dynamics and Chaos* (Addison-Wesley, Reading, MA, 1994).
- [29] C. Radehaus, R. Dohmen, H. Willebrand, and F.-J. Niedernostheide, *Phys. Rev. A* **42**, 7426 (1990).
- [30] H.-G. Purwins, C. Radehaus, T. Dirksmeyer, R. Dohmen, R. Schmeling, and H. Willebrand, *Phys. Lett. A* **136**, 480 (1989).
- [31] P. Schütz, diploma thesis, Münster University, 1990 (unpublished).
- [32] J. Meunier, P. Belenguer, and J. P. Boeuf, *J. Appl. Phys.* **78**, 731 (1995).
- [33] I. Brauer, C. Punset, H.-G. Purwins, and J. P. Boeuf, *J. Appl. Phys.* **85**, 7569 (1999).